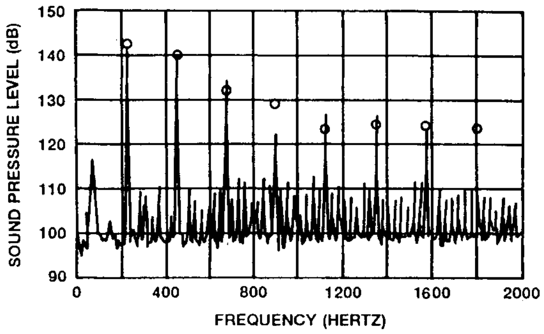

Fig. 5 Spectrum comparison at 0.25 diameter aft: ⊙, present theory corrected for amplification at boom.

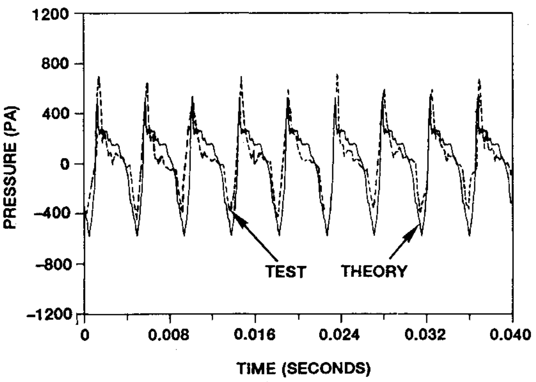

Fig. 6 Waveform comparisons for 1-deg downtilt at 0.25 diameter aft, not corrected for boom amplification.

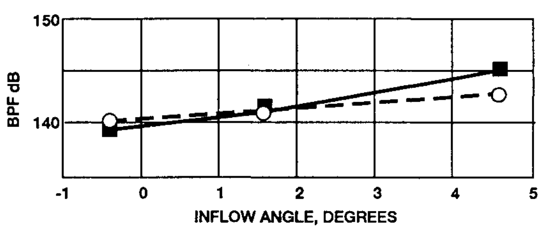

Fig. 7 Effect of nacelle tilt at 0.25 diameter aft: ■, data correct to free field; ○, present theory.

explain the discrepancy. Possible reasons include nonlinear propagation, reflection from the fuselage, and inadequate estimates of loading. Also, Farassat et al.[8] have noticed that measured noise directivity patterns on the fuselage suggest that the level of the forward microphone should be several dB higher. Since the agreement is good at the 0.25*D* aft position, the remaining figures address that microphone. Figure 5 shows that agreement with the upper harmonics at this location are excellent. (Here the boom corrections with Ref. 6 for the first four harmonics were 0.7, 3.1, 3.9, and 3.4 dB. The higher harmonics had to be estimated at 4.0 The waveform in Fig. 6 was generated using 15 harmonics. Agreement is good enough to indicate that the theory represents the physics properly. Finally, Fig. 7 shows trends with nacelle tilt at BPF. The new method predicts levels reasonably accurately, although the trend with tilt is weaker than that of the data.

Conclusions

A new theoretical method has been presented for prediction of harmonic noise of open rotors. By use of a numerical source integration, the method can account directly for effects such as shaft tilt, radial loading, unsteady volume displacement, and placement of the sources on the blade's actual camber surface. Fore and aft directivity predictions are moderately good, with deviations attributable possibly to nonlinear propagation or source effects and neglect of effects of testing on a real airplane such as reflections from the aircraft. It is hoped that further studies in progress with the new method will shed light on these issues.

References

[1]Bartel, H. W., and Swift, G., "Near-Field Acoustic Characteristics of a Single-Rotor Propfan," AIAA Paper 89-1055, April 1989.

[2]Nallasamy, M., Envia, E., Clark, B. J., and Groeneweg, J. F., "Near-Field Noise of a Single Rotation Propfan at an Angle of Attack," AIAA Paper 90-3953, Oct. 1990.

[3]Hanson, D. B., "Near-Field Frequency-Domain Theory for Propeller Noise," *AIAA Journal*, Vol. 23, No. 4, 1985, pp. 499–504.

[4]Hanson, D. B., "Unified Aeroacoustic Analysis for High Speed Turboprop Aerodynamics and Noise," NASA CR-4329, March 1991.

[5]Envia, E., private communication, April 1991.

[6]Hanson, D. B., and Magliozzi, B., "Propagation of Propeller Tone Noise Through a Fuselage Boundary Layer," *Journal of Aircraft*, Vol. 22, No. 1, 1985, pp. 63–70.

[7]Garrick, I. E., and Watkins, C. E., "A Theoretical Study of the Effect of Forward Speed on the Free-Space Sound-Pressure Field Around Propellers," NACA Rept. 1198, 1953.

[8]Farassat, F., Dunn, M. H., and Spence, P. L., "Advanced Propeller Noise Prediction in the Time Domain," *AIAA Journal,* Vol. 30, No. 9, 1992, pp. 2337–2340.

[9]Hanson, D. B., "Noise Radiation of Propeller Loading Sources with Angular Inflow," AIAA Paper 90-3995, Oct. 1990.

Advanced Propeller Noise Prediction in the Time Domain

F. Farassat*
NASA Langley Research Center,
Hampton, Virginia 23665
and
M. H. Dunn† and P. L. Spence‡
Lockheed Engineering & Sciences Company,
Hampton, Virginia 23666

Introduction

In a recent paper,[1] results from two frequency domain methods for predicting high-speed propeller noise by Hanson[2,3] and Envia (unpublished) were presented together with comparison with measured data. One of the objectives of the paper was to study the nonaxial inflow effect. The calculations by Hanson's method were performed using a computer code identified as frequency domain, Hanson (FDH) that does not account for nonaxial inflow effects. The acoustic code based on Envia's theory, identified as frequency domain, Envia (FDE), includes these effects. In Ref. 1, the measured acoustic data used for comparison with predictions were supplied by the Propeller Test Assessment (PTA) aircraft. This aircraft has a 2.74 m (9 ft) diameter, eight-bladed advanced propeller

Received Oct. 28, 1991; revision received Dec. 10, 1991; accepted for publication Dec. 27, 1991.

*Senior Research Scientist, Applied Acoustics Branch. Associate Fellow AIAA.

†Principal Engineer, Acoustics and Dynamics Department, 144 Research Drive. Member AIAA.

‡Senior Engineer, Acoustics and Dynamics Department, 144 Research Drive. Member AIAA.

(SR-7L) with a design flight Mach number of 0.8. Some near-field acoustic data and operating conditions for this propeller were presented by Bartel and Swift.[4] The nacelle tilt in the PTA aircraft could be set to three pitch angles to evaluate the nonaxial inflow effect.

Hanson's most recent frequency domain method for the far field includes the effect of the nonaxial inflow on noise.[5] A near-field version of the theory is presented in an accompanying Note by Hanson.[6] As mentioned there, a minor error in Envia's code invalidated the calculations in Ref. 1. The purpose of the present Note is to bring to the attention of readers a similar theory in the time domain and the computer code ASSPIN that includes the effect of nonaxial inflow on propeller noise.

Noise Theory and the Computer Code ASSPIN

Since the mid-1970s, several acoustic formulations for prediction of noise of rotating blades in the time domain have been derived by Farassat. Two of these[7,8] are now used exclusively in various computer codes developed at NASA Langley Research Center for helicopter rotors and propellers. A computer code for advanced propeller noise prediction based on these two formulations known as DFP-ATP was developed by Farassat et al.[9] This code assumes axial inflow to the propeller.

The two acoustic formulations are solutions of the Ffowcs Williams-Hawkings equation (without the quadrupole term) using the Green's function approach. They are in the form of line and surface integrals over panels on the propeller surface that are evaluated numerically. One of the major characteristics of the time domain method is that these two formulations are valid in the near and far fields and also for nonaxial inflow to the propeller. Furthermore, they utilize exact blade geometry and kinematics. By using algorithmic changes in retarded time calculations, the computer code DFP-ATP was modified to include the nonaxial inflow effect. In addition, two new features—adaptive time steps and a periodic loading noise option—were introduced in the code. This new code is now called the Advanced Subsonic and Supersonic Propeller Induced Noise (ASSPIN) noise prediction program.

Current advanced propellers are very thin near the tip, and they operate at high load factors so that blade deformation has noticeable effects on propeller aerodynamics and noise. The comprehensive propeller noise prediction program of NASA Langley was developed specifically to study these effects. Four state-of-the-art codes for aeroelasticity (NASTRAN), propeller aerodynamics (Celestina et al.[10]), propeller acoustics code (DFP-ATP/ASSPIN), and boundary-layer propagation code (MRS-BLP)[11] were interfaced for automatic execution on a computer.[12] Because aerodynamics and aeroelasticity are coupled phenomena, an iterative scheme between the aeroelastic and aerodynamic codes is employed to obtain the hot (i.e., deformed) blade coordinates and blade surface pressure. In the noise calculations below, the effect of blade deformation by mean blade loading on the predicted noise is included.

Comparison with Measured Data

In this section, predictions similar to those of Hanson[6] for a nacelle tilt of − 1 deg will be presented and compared with measured data. Because the exact data used by Hanson for blade loading and geometry were unavailable to the authors, the predictions here utilize blade unsteady aerodynamic results from Whitfield's code supplied by Nallasamy et al.[1] The blade deformation is obtained from iterations between the NASTRAN code and that of Celestina et al.[10] based on the mean loading corresponding to − 1 deg nacelle tilt. These differences in input data explain the discrepancies between the present predictions by ASSPIN and those from Hanson's code.[1,6] Previous comparisons of the two codes with identical input data gave remarkable agreement among computed spectra (within 0.5 dB for most harmonics).

All of the predictions of this Note for axial inflow are for condition 350 of the PTA aircraft (flight Mach number = 0.800, helical tip Mach number = 1.136, shaft horsepower = 3072, nacelle tilt = 1 deg down). The boom scattering corrections, given in Table 1, were calculated from MRS-BLP[11] using the boom diameter at each microphone location. The boom is 0.62 propeller diameter from the disk center and parallel to the fuselage centerline. Figure 1 shows the measured and predicted levels of BPF for the five boom microphone positions. The test data in this figure have been corrected to free field values using boom scattering corrections. Note that the axial boom microphone locations can be read from this figure with microphone 1 ahead of the propeller disk. In this figure the flow is assumed uniform in the prediction but the blade surface pressure is unsteady. This figure must be compared with Fig. 1 of Ref. 6. As seen from these figures, both ASSPIN and Hanson's code overpredict for microphones 1 and 5. There is some evidence that microphone 1 was not functioning correctly during the tests.[12] ASSPIN's result for microphone 2 (in plane) agrees better with measured data than that from Hanson's code. For microphone 3, ASSPIN underpredicts measured data by about 2 dB whereas Hanson's result agrees well with measured data. For microphone 4 both codes do well. Microphone 5 is probably influenced by proximity of wing and nacelle surfaces.

Figure 2, corresponding to Fig. 4 of Ref. 6, shows that the inclusion of nonaxial inflow effect improves the agreement between measured and predicted data by ASSPIN for microphone 3. Other microphone locations are not influenced substantially. Hanson's code shows that the predicted data are influenced at all microphones except microphone 3. Note that Hanson's input data differ from those used by Nallasamy et al.[1] and those used in this Note.

Figure 3, corresponding to Fig. 5 of Ref. 6, shows the comparison of measured and predicted acoustic spectra for

Table 1 Boom microphone scattering corrections—condition 350

	Boom, dB				
	1	2	3	4	5
1 × BPF[a]	− 0.1	1.0	1.1	0.5	0.8
2 × BPF	—	3.5	3.9	3.0	—
3 × BPF	—	5.4	4.6	3.6	—
4 × BPF	—	6.0	6.0	6.0	—
5 × BPF	—	6.0	6.0	6.0	—
6 × BPF	—	6.0	6.0	6.0	—
7 × BPF	—	6.0	6.0	6.0	—
8 × BPF	—	6.0	6.0	6.0	—

[a]Blade passing frequency.

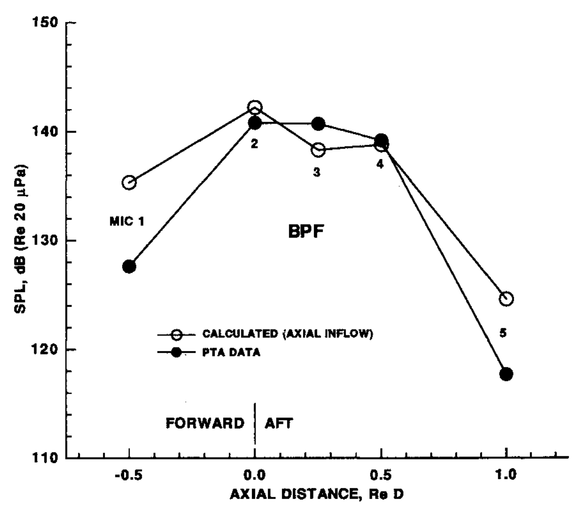

Fig. 1 Noise levels along microphone boom at a constant sideline distance of 0.62 diameter, PTA data corrected to free field.

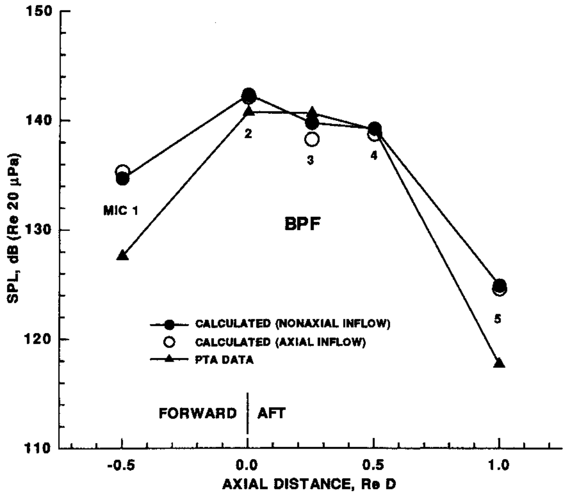

Fig. 2 Directivity along microphone boom for 1 deg downtilt, PTA data corrected to free field.

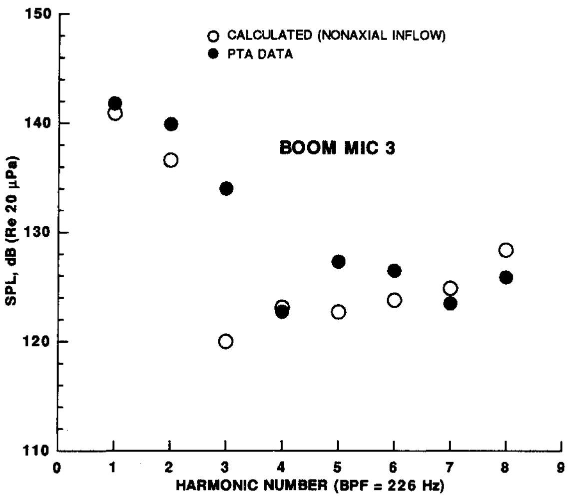

Fig. 3 Spectrum comparison at boom microphone 3 (0.25 diameter aft), scattering corrections added to predicted results.

boom microphone 3. In this figure, boom scattering corrections from Table 1 have been added to the predicted levels of the spectrum. Although Hanson's code gives good agreement at all harmonics, ASSPIN underpredicts at second, third, fifth, and sixth harmonics and there is slight overprediction at seventh and eighth harmonics. The reason for considerable underprediction in the third harmonic is the sensitivity to the blade loading at this microphone location. The interaction between the phase of thickness and loading noise produces destructive interference at the third harmonic. Figure 4 shows the measured and predicted acoustic spectra from ASSPIN for boom microphone 2 with good agreement between the two data. Boom scattering corrections have been added to the predicted data. Figure 5, corresponding to Fig. 6 of Ref. 6, shows the measured and predicted acoustic pressure signatures by ASSPIN for boom microphone 3. Note that no boom scattering correction has been applied to predicted signature. The effect of boom scattering is more pronounced at high harmonics. There is good agreement between the measured and predicted signatures from ASSPIN and Hanson's code.

Figure 6, corresponding to Fig. 7 of Ref. 6, shows the variation of the levels of blade passing frequency (BPF) at boom microphone 3 with inflow angle variation using ASSPIN. PTA data exist for three inflow angles—0.4 deg down, 1.6 deg up, and 4.6 deg up—corresponding to three nacelle tilt angles: 3 deg down, 1 deg down, and 2 deg up. The inflow angles, which are functions of aircraft angle of attack, propeller upwash angle, and nacelle tilt, were estimated by Nallasamy et al.[1] The prediction for the inflow angle of 0.4 deg down corresponds to condition 806 of the PTA aircraft (flight Mach number = 0.809, helical tip Mach number = 1.140, shaft horsepower = 3008, nacelle tilt = 3 deg down). The 1.6 deg up inflow angle case corresponds to condition 350, and the 4.6 deg up inflow angle case is associated with condition 935 of the PTA aircraft (flight Mach number = 0.811, helical tip Mach number = 1.150, shaft horsepower = 3024, nacelle tilt = 2 deg up). Although there is some underprediction at all nacelle tilts, the trend of measured data is predicted accurately. The best agreement is at small positive inflow angle for both codes. In general, both codes show that they can reliably predict the trends and acoustic levels due to nonaxial inflow.

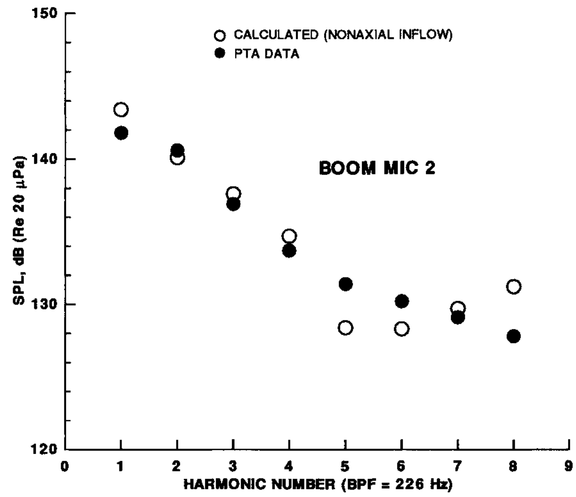

Fig. 4 Spectrum comparison at boom microphone 2 (plane of propeller), scattering corrections added to predicted results.

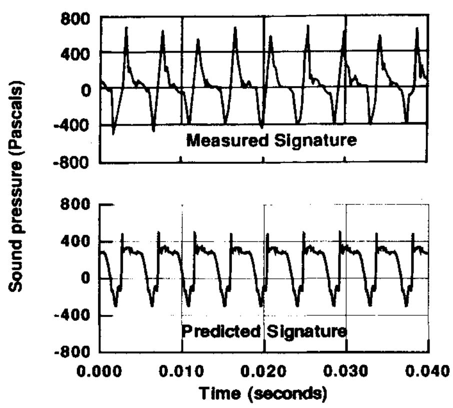

Fig. 5 Pressure signature comparison for 1 deg downtilt at boom microphone 3 (0.25 diameter aft), predicted results not corrected for boom scattering.

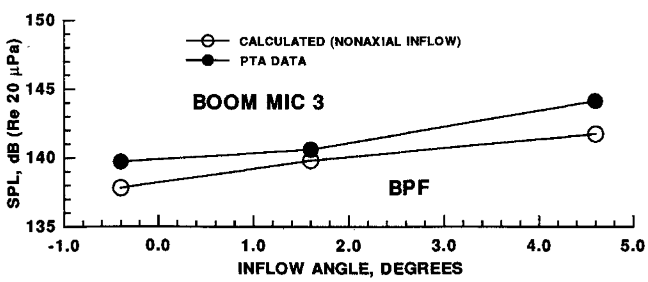

Fig. 6 Effect of nacelle tilt at boom microphone 3 (0.25 diameter aft), PTA data corrected to free field.

Conclusions

The time domain code ASSPIN provides acousticians with a powerful method of advanced propeller noise prediction. With the exception of nonlinear effects, the code utilizes exact solutions of the Ffowcs Williams-Hawkings equation with exact blade geometry and kinematics. With the inclusion of nonaxial inflow, periodic loading noise, and adaptive time steps to speed up computer execution, the development of this code is now complete. It is important to recognize that correct blade coordinates and loads must be obtained by iteration between an aeroelastic and an aerodynamic code. In addition, the effects of other acoustic phenomena, such as reflections from wing, nacelle, and fuselage, in aircraft tests must be included in comparisons of measured and predicted noise data.

References

[1]Nallasamy, M., Envia, E., Clark, B. J., and Groeneweg, J. F., "Near-Field Noise of a Single Rotation Propfan at an Angle of Attack," AIAA Paper 90-3953, Oct. 1990.

[2]Hanson, D. B., "Near-Field Frequency-Domain Theory for Propeller Noise," *AIAA Journal,* Vol. 23, No. 4, 1985, pp. 499–504.

[3]Hanson, D. B., "Unified Aeroacoustic Analysis for High Speed Turboprop Aerodynamics and Noise," NASA CR-4329, March 1991.

[4]Bartel, H. W., and Swift, G., "Near-Field Acoustic Characteristics of a Single-Rotor Propfan," AIAA Paper 89-1055, April 1989.

[5]Hanson, D. B., "Noise Radiation of Propeller Loading Sources with Angular Inflow," AIAA Paper 90-3955, Oct. 1990.

[6]Hanson, D. B., "Direct Frequency Domain Calculation of Open Rotor Noise," *AIAA Journal,* Vol. 30, No. 9, 1992, pp. 2334–2337.

[7]Farassat, F., and Succi, G. P., "The Prediction of Helicopter Rotor Discrete Frequency Noise," *Vertica,* Vol. 7, No. 4, 1983, pp. 309–320.

[8]Farassat, F., "Theoretical Analysis of Linearized Acoustics and Aerodynamics of Advanced Supersonic Propellers," *Aerodynamics and Acoustics of Propellers,* AGARD CP-366(10), 1985, pp. 1–15.

[9]Farassat, F., Padula, S. L., and Dunn, M. H., "Advanced Turboprop Noise Prediction Based on Recent Theoretical Results," *Journal of Sound and Vibration,* Vol. 119, 1987, pp. 53–79.

[10]Celestina, M. L., Mulac, R. A., and Adamczyk, J. J., "A Numerical Simulation of the Inviscid Flow Through a Counter-Rotating Propeller," *Transactions of the ASME, Journal of Turbomachinery,* Vol. 108, 1986, pp. 187–193.

[11]Spence, P. L., "Development of a Boundary Layer Noise Propagation Code and Its Application to Advanced Propellers," AIAA Paper 91-0593, Jan. 1991.

[12]Dunn, M. H., and Farassat, F., "High-Speed Propeller Noise Prediction—A Multidisciplinary Approach," *AIAA Journal,* Vol. 30, No. 7, 1992, pp. 1716–1723; also AIAA Paper 90-3934.

Comparison of Transonic Flow Models

Kevin McGrattan*
New York University, New York, New York 10003

Introduction

DURING the past 10 years, there has been much discussion of the relative merits of the potential and the Euler formulations of the equations of motion of transonic flow over supercritical wing sections. To study the two models in a common framework, a finite difference version of the Euler solver[1] has been incorporated into the potential code that is described in Ref. 2. The purpose of this Note is to highlight some of the more interesting discoveries of the study.

First, the Euler solver is less reliable than the potential solver in predicting the wave drag. For computations of the Euler equations with a boundary-layer correction, the standard pressure integration around the airfoil is faulty due to the inaccuracy of the flow variables in the wake. As a possible alternative, the Euler equations modified by artificial viscosity terms can be combined to form an equation for the entropy whose viscous terms provide a means of calculating the wave drag. Instead of differencing uncertain values of pressure at the tail and the nose, a positive definite quantity is integrated over the region surrounding a shock.

For flows with relatively weak shocks, there is little difference between the Euler and the potential models because the jump in entropy across a shock is of third order in the shock strength. This suggests that in cases with weak shocks, there should exist nonunique solutions of the Euler equations where there exist nonunique solutions of the potential equations. References 3 and 4 present nonunique solutions of the potential equation for airfoils at relatively high Mach numbers with strong shocks. The authors claim that the phenomenon is related to the isentropic assumption of the potential model. However, a thin, supercritical airfoil will be presented which not only yields a nonunique potential solution, but also a nonunique Euler solution.

Wave Drag and the Entropy Inequality

The Euler solver described in Ref. 1 employs central differences for all spatial derivatives, and therefore explicit artificial viscosity terms must be added to all four equations in order to guarantee convergence. A check on the physical validity of the additional terms is to show that the entropy inequality is satisfied by the modified equations. From this an alternative method of computing wave drag may be derived following the idea presented in Ref. 5. This calculation involves the summing of a positive definite quantity over the region of the flow in which the shock is smeared, avoiding the use of computed flow variables near the tail which are subject to great uncertainty when a boundary-layer correction is included.

Consider the Euler equations modified by the second-order artificial viscosity terms:

$$\rho_t + (\rho u)_x + (\rho v)_y = \nabla \cdot \nu \nabla \rho \tag{1a}$$

$$(\rho u)_t + (\rho u^2 + p)_x + (\rho u v)_y = \nabla \cdot \nu \nabla (\rho u) \tag{1b}$$

$$(\rho v)_t + (\rho u v)_x + (\rho v^2 + p)_y = \nabla \cdot \nu \nabla (\rho v) \tag{1c}$$

$$(\rho E)_t + (\rho u H)_x + (\rho v H)_y = \nabla \cdot \nu \nabla (\rho H) \tag{1d}$$

where the artificial viscosity operator is defined as

$$\nabla \cdot \nu \nabla \equiv \frac{\partial}{\partial x}\left(\nu^{(x)} \frac{\partial}{\partial x}\right) + \frac{\partial}{\partial y}\left(\nu^{(y)} \frac{\partial}{\partial y}\right)$$

These four equations may be combined to form a fifth equation for the entropy

$$(\rho S)_t + (\rho u S)_x + (\rho v S)_y = \frac{c_v \rho}{e} \| w \|^2_{WD} + \nabla \cdot \nu \left\{ S \nabla \rho + \frac{c_v \rho \nabla e}{e} + \frac{c_v \nabla p}{e} \right\} \tag{2}$$

The positive definite wave-drag norm is defined as

$$\| w \|^2_{WD} = \| \nabla u \|^2 + \| \nabla v \|^2 + \gamma e \left(\left\| \frac{\nabla p}{p} \right\|^2 - \frac{\gamma + 1}{\gamma} \left\langle \frac{\nabla p}{p}, \frac{\nabla \rho}{\rho} \right\rangle + \left\| \frac{\nabla \rho}{\rho} \right\|^2 \right)$$

Received Sept. 17, 1991; revision received Dec. 16, 1991; accepted for publication Dec. 17, 1991.

*Courant Institute of Mathematical Sciences; currently at National Inst. of Standards and Technology, Gaithersburg, MD 20899.